

# Performance Analysis of Advanced GPS Receiver Technique in Radio Frequency Difficult Environment \*

Li-Ta Hsu \*\* and Shau-Shiun Jan

*Department of Aeronautics and Astronautics, National Cheng Kung University  
No.1, University Road, Tainan City 701, Taiwan, R.O.C.*

## ABSTRACT

Global Positioning System (GPS) is widely used in many applications, especially on its position, velocity and timing (PVT) services. In general, a GPS receiver performs accurately and smoothly under open-sky environment. However, under urban canyon and dense foliage environments, a GPS receiver could not provide PVT services adequately due to GPS signal blockage or multipath. As a result, this paper develops and implements an advance GPS receiver technique, the Vector Tracking (VT) technique, to compare its performance with the conventional standard GPS receiver design under radio frequency difficult environments. The VT technique is based on an Extended Kalman Filter (EKF) to track all GPS satellites simultaneously and to estimate the user's position, velocity, and clock bias. The VT technique takes the advantage of the user's dynamic to predict the associated changes in the GPS signal, and it could thus facilitate the GPS receiver to bridge the temporary signal outages. Additionally, the tuning of the EKF is the key performance factor of the VT technique, and two algorithms to estimate the noise covariance, namely the correlation method and the empirical setting method, are discussed in this paper as well. Finally, this paper presents the performance gained from the developed VT technique in comparison to the conventional GPS receiver under various Radio Frequency (RF) difficult environments.

**Keywords:** GPS, Extended Kalman filter (EKF), Vector tracking, Parameter tuning

## I. INTRODUCTION

Global Positioning System (GPS) provides the navigation, positioning, and timing service to numerous applications. This makes the GPS indispensable in modern society. According to the research report, the total GPS market is expected to reach \$26.67 billion by 2016 [1] As the requirement of GPS keeps growing, the reliability of GPS navigator became an essential factor, especially on the Radio Frequency (RF) difficult environments. These RF difficult environments, such as tunnel and urban canyon, might block or reflect the GPS signal to reduce the stabilities and performance of GPS receivers [2]. In this paper, the Tzu-Chiang Campus of

National Cheng Kung University in Taiwan is selected as the experiment field as shown in Figure 1. It is difficult for a user surrounded by the high buildings and the street trees to receive good GPS signal to navigate. Thus, Spilker and Parkinson proposed the idea of the vector tracking [3]. The conventional tracking method tracks each satellite with independent channels. The major difference between the conventional tracking method and the vector tracking is that the latter utilizes an Extended Kalman Filter (EKF) to track all satellites jointly. Pany et al. pointed out that this characteristic benefits the receiver with availability and accurate Doppler frequency and pseudorange [4]. Recently, Zhao et al. released an open source for implementing a vector tracking loop to a

\* Manuscript received, September 1, 2013, final revision, September 2, 2013

\*\* To whom correspondence should be addressed, E-mail: ssjan@mail.ncku.edu.tw

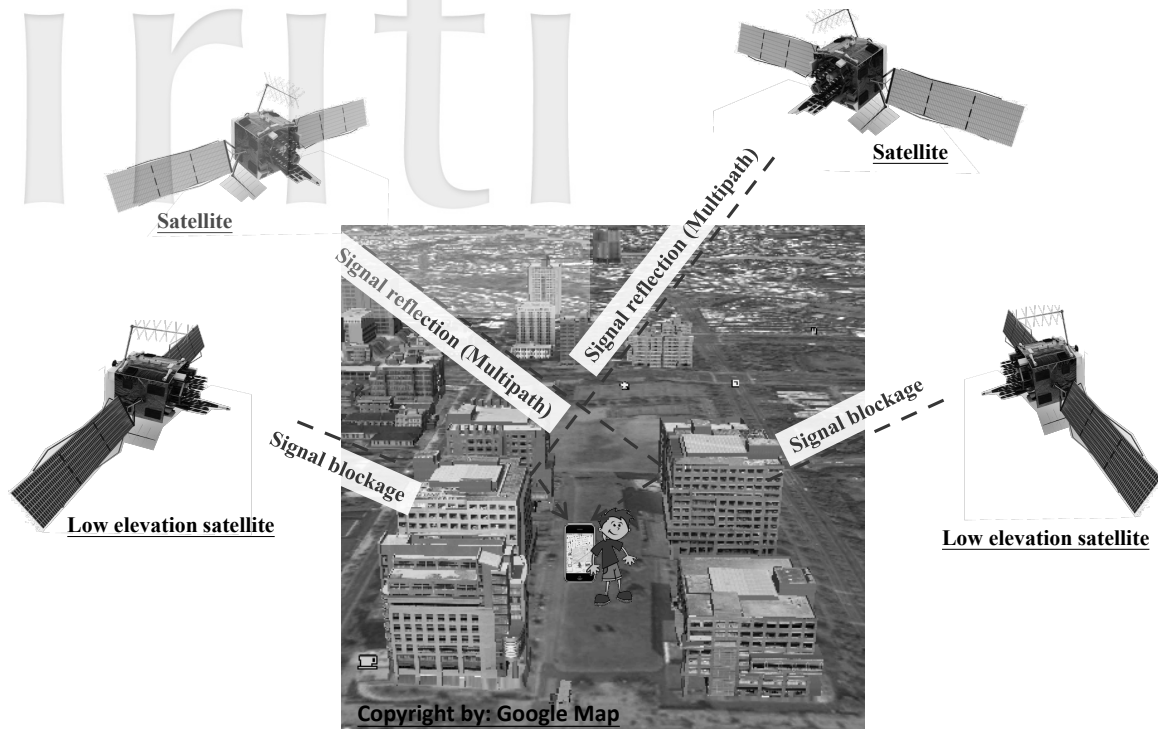


Figure 1 An illustration of the reflection and the blockage of GPS signal due to the radio difficult environment. This field is the Tzu-Chiang Campus of National Cheng Kung University in Taiwan which is selected as the experiment field in this paper

software receiver [5]. By means of this release, the detail of the vector tracking is finally revealed. The objective of this paper is to investigate the benefit of the vector tracking and to study the noise calibration of the EKF of the vector receiver. However, the automatic tuning of the vector tracking is seldom mentioned. The most common mentioned noise calibration method of Kalman filter is the empirical tuning method. This tuning method is usually applied by trial and error approach. Although the performance of the empirical tuning method is generally stable, it requires a huge amount of time to refine a tuning for a specific dataset. For different dynamic scenarios, the noise covariance value has to be calibrated again. In addition, the calibration becomes more complicated when the number of states increased. To reduce the heavy workload of tuning the noise covariance, this paper attempts to implement an automatic calibration process to the vector tracking technique. A calibration method called, the correlation method, which might be a candidate due to its applicability to constant coefficient systems, and it correlates the outputs of a system to estimate the unknown parameters. The details of the correlation method will be described in section III.

## II. VECTOR TRACKING

### Architecture and Algorithm

The conventional tracking (CT) technique tracks the signals from different satellites independently. The potential linkages between satellites are totally ignored. In comparison to the conventional tracking, the vector

tracking (VT) can aggregate signal powers from all channels. This characteristic enables the vector tracking to mitigate the effect of the short outage of signals. In general, the vector tracking could be branched into two categories: Vector Delay Lock Loop (VDLL), and Vector Delay and Frequency Lock Loop (VDFLL). This paper focuses on the VDLL. To utilize the VDLL, the initialization from the conventional tracking is required. The required initialization includes the code frequency, Doppler frequency, user position/velocity, and the satellite ephemeris. After obtaining the information from the conventional receiver, the VDLL could be executed. The overall architecture of the VDLL utilized in this paper is shown in Figure 2. The VDLL technique replaces the Delay Lock Loop (DLL) by using the estimated user information to predict the code frequency and to lock the code phase, and it preserves the Phase Lock Loop (PLL) to lock the carrier phase. The detailed procedures of the VDLL are given below.

#### Initialization:

In the CT process, the initial code phase and Doppler frequency are given by the acquisition process. The VT technique employs the CT technique for its initialization. The required initialization includes the code frequency, Doppler frequency, user position/velocity, and the satellite ephemeris.

#### STEP 1: Integration and dumping

The initialized or estimated code/carrier frequency is used to generate the signal replicas. Once the replicas are obtained, the correlations between different replicas and

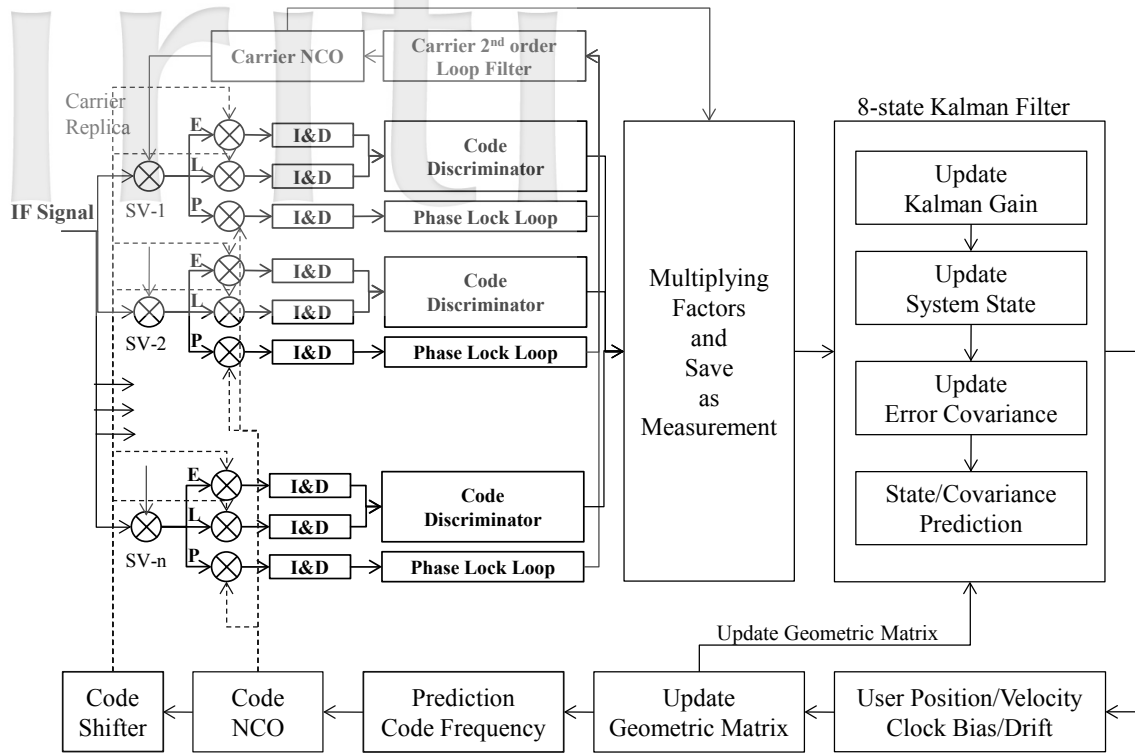


Figure 2 The overall flowchart of the VDLL implemented in this paper

the intermediate frequency (IF) signal are calculated and sent to the code/carrier discriminators.

#### STEP 2: Measurements

The code/carrier discriminator outputs are calculated using the correlation value. In this paper, the selected carrier phase arctangent typed discriminator ATAN(Q/I) and the loop filter is a 2nd order loop filter [6]. Thus, the Doppler frequency can be obtained using PLL. With regards to the code discriminator, normally, the “early minus late discriminator” will be utilized to distinguish the degree of shifted code [6]. Once the code discriminator output and Doppler frequency are estimated, they have to be transformed into the delta pseudorange and the Doppler velocity, respectively, in order to estimate the user information. The transformations are:

$$\rho_j = \text{code discrim} \times \frac{c}{f_0} \quad (1)$$

$$v_j = \text{Doppler freq}_j \times \frac{c}{f_{L1}} \quad (2)$$

where  $\Delta\rho_j$  and  $v_j$  are the delta pseudorange and Doppler velocity, respectively.  $\text{code discrim}_j$  and  $\text{Doppler freq}_j$  are code discriminator output and Doppler frequency, respectively.  $c$  is the light speed,  $f_0$  is the chipping rate (1.023 MHz for GPS C/A code), and  $f_{L1}$  is the L1 band frequency (1575.42 MHz for GPS L1 signal).

#### STEP 3: Calculation of user information by EKF

The EKF implemented in this paper consists of two stages, namely update and prediction. Equations of the EKF utilized in this paper are:

Update:

$$K_k = P_k^- H_k^T [H_k P_k^- H_k^T + R_k]^{-1} \quad (3)$$

$$\hat{X}_k^+ = \hat{X}_k^- + K_k [Z_k - H_k \hat{X}_k^-] \quad (4)$$

$$P_k^+ = [I - K_k H_k] P_k^- \quad (5)$$

Prediction:

$$\hat{X}_{k+1}^- = \Phi_k \hat{X}_k^+ \quad (6)$$

$$P_{k+1}^- = \Phi_k P_k^+ \Phi_k^T + Q_k \quad (7)$$

The subscript  $k$  indicates the epoch and superscripts +/- represent predicted and non-predicted information, respectively.  $\hat{X}$  is the state,  $Z$  is the measurement,  $K$  is the Kalman gain,  $P_k^-$  is the state covariance,  $H$  is the observation matrix,  $\Phi$  is the dynamic model, and  $R$  and  $Q$  are the noise covariances of the measurement and process, respectively. The system states utilized in this paper are composed of the change of the user position/velocity in 3 dimensions and the change of the user clock bias/drift (i.e., 8 states in total):

$$X = [\delta P_{1 \times 3} \quad \delta V_{1 \times 3} \quad \delta B_{1 \times 2}]^T_{1 \times 11} \quad (8)$$

The system dynamic model is:

$$\Phi = \begin{bmatrix} 0_{3 \times 3} & I_{3 \times 3} & 0_{3 \times 2} \\ 0_{3 \times 3} & 0_{3 \times 3} & 0_{3 \times 2} \\ 0_{2 \times 3} & 0_{2 \times 3} & \Phi_{clk} \end{bmatrix}_{8 \times 8} \quad \Phi_{clk} = \begin{bmatrix} 0 & 1 \\ 0 & 0 \end{bmatrix} \quad (9)$$

The measurements applied in the EKF are the code discriminator output and Doppler frequency from each channel:

$$Z = \begin{bmatrix} \text{code disc}_i, \text{Doppler freq}_i \\ \vdots \\ \text{code disc}_j, \text{Doppler freq}_j \end{bmatrix} \times \begin{bmatrix} c/f_0 & 0 \\ 0 & c/f_{L1} \end{bmatrix} \quad (10)$$

The relation between the state and measurement is called the observation matrix:

$$H = \begin{bmatrix} a_x^1 & a_y^1 & a_z^1 & 0_{1 \times 3} & 1 & 0 \\ & & \vdots & & & \\ a_x^j & a_y^j & a_z^j & 0_{1 \times 3} & 1 & 0 \\ 0_{1 \times 3} & -a_x^1 & -a_y^1 & -a_z^1 & 0 & -1 \\ & & \vdots & & & \\ 0_{1 \times 3} & -a_x^j & -a_y^j & -a_z^j & 0 & -1 \end{bmatrix}_{2j \times 8} \quad (11)$$

where  $[a_x^j \ a_y^j \ a_z^j]$  represents the line of sight (LOS) vector between the estimated user position and the satellite  $j$ . The first step of the EKF process is to compute the Kalman gain by fusing the state noise covariance and the measurement noise covariance. The updated state and its variance are then calculated from the measurement. Finally, the user information is predicted using the system dynamic model. Details of the Kalman filter process can be found in [7]. The algorithm of estimating the measurement and process noise covariances utilized in this paper is an adaptive method. The basic idea is to correlate the output and to derive the system parameters using the autocorrelation function. Details of the correlation method can be found in the next section. The second approach for estimating the noise covariance is setting the value from the empirical experience.

#### STEP 4: Prediction of the signal parameter

The EKF is used to obtain the user position/velocity and clock bias/drift. These estimations provide sufficient information to predict the code frequency for the next epoch. The concept of the code frequency is based on the Doppler effect between the satellite vehicle (SV) and user. The equation of the predicted code frequency is:

$$\hat{f}_{code,j,k+1} = \left[ 1 + \frac{t_{d,k}}{c} + \frac{(V_{j,k} - v_k)^T a_{j,k+1}}{c} \right] f_{code,j,k} \quad (12)$$

where  $t_{d,k}$  is the user clock bias at epoch  $k$ ,  $V_{j,k}$  is the velocity of SV  $j$ ,  $v_k$  is the user velocity,  $a_{j,k+1}$  is the LOS vector between the estimated user position and satellite  $j$ , and  $f_{code,j,k}$  is the code frequency at epoch  $k$ .

#### STEP 5: Generation of the code/carrier replicas

The carrier phase and Doppler frequency are obtained using the PLL (in STEP 2), and the code frequency is obtained using prediction (in STEP 5). The signal replicas are thus generated. The signal replicas are fed back to STEP 1 and the procedure is repeated.

### III. NOISE CALIBRATION

#### Empirical Tuning

The noise calibration of the vector tracking is a key factor to track satellite signal successfully. The most common noise calibration method is to tune the measurement ( $R$ ), the process noise covariance ( $Q$ ), and the initial state noise covariance ( $P$ ) empirically. In general, the empirical tuning is to manually alter the value of  $P$ ,  $Q$ , and  $R$  by the trial and error testing. It would be a challenge to change these noise covariances simultaneously due to that there are several undetermined parameters. One should note that the most crucial performance parameter of Kalman filter is the ratio of the state error and measurement noise covariance matrices ( $P/R$ ) [7]. If the setting of  $P/R$  is too small, the Kalman filter will converge in a slow fashion than it required. Conversely, if the  $P/R$  is overestimated, the Kalman filter would over believe the measurement noise which might result in a rapid diverge from the truth. In general, the state noise matrix is first set by predicting the error of state per epoch, then tuning the measurement noise matrix until the Kalman filter converged. With the respect of tuning the process noise matrix, it is based on the prediction of possible state error during the each estimation. The settings of clock bias and drift are based on the resolution of numerically controlled oscillator (NCO) and NCO rate, respectively. The calculations of the resolutions for software receiver are addressed below [8]:

$$\Delta\phi \text{ (unit: samples)} = 1/2^m o \quad (13)$$

$$\Delta\dot{\phi} \text{ (unit: } \frac{\text{samples}}{\text{sec}}) = f_s / o 2^m \quad (14)$$

where  $m$  is the number of bits of the operation system (32 bits used in this paper),  $o$  is the oversample factor (i.e., samples for a chip).

#### Correlation Method

Unlike the empirical tuning method, the correlation

method could estimate the measurement and process noise covariance automatically. The basic idea of the correlation method is to correlate the system output to derive the system parameters [9]. This correlation method is widely used in time series analysis. In addition, this method could generate the unbiased and consistent estimates for time-invariant system. This paper assumes the tracking system is stationary and time-invariant. The correlation of the system output  $z$  is:

$$C_{k+1} = E\{z_i z_{i-k}^T\} = \begin{cases} H\Sigma H^T + R & k = 0 \\ H\Phi^k \Sigma H^T & k > 0 \end{cases} \quad (15)$$

where  $x$  is the system state,  $z$  is the system output,  $k$  is the epoch,  $H$  is the observation matrix, and  $\Phi$  is the state transition matrix,  $\Sigma = \lim_{k \rightarrow \infty} E\{x_k x_k^T\}$  which satisfied:

$$\Sigma = \Phi \Sigma \Phi^T + Q \quad (16)$$

Then, the second case of Eq. (15) can be reorganized to Eq. (17) for  $k = 1$  to  $n$ ,

$$[C_1 \ \dots \ C_n]^T = A \Sigma H^T \quad (17)$$

where  $A = [\Phi^T H^T \ \dots \ (\Phi^T)^n H^T]$  and  $n$  is totally number of epoch used to estimate the noise covariance. Due to the state transition matrix is nonsingular and observable, the existence of inverse of  $A^T A$  is guaranteed. Finally, the  $R$  and  $Q$  could be estimated by setting  $k=0$  on Eq. (15) and reorganized Eq. (16), respectively.

$$R = C_0 - H \Sigma H^T \quad (18)$$

$$Q = \Sigma - \Phi \Sigma \Phi^T \quad (19)$$

The initial state error matrix is not being estimated in the correlation method, hence, the empirical value is used. In this paper,  $n$  is selected to be 1,000 epochs. In the period of accumulating total epochs for the correlation method, the setting of  $Q$  and  $R$  of the empirical tuning method are applied.

#### IV. EXPERIMENTAL RESULTS

##### Comparison between Conventional Receiver and Vector Receiver

This paper first utilizes a commercial GPS receiver, Garmin GPS 35, to test the selected experimental field. The test result is shown in Figure 3. As shown in Figure 3, the average Geometric Dilution of Precision (GDOP) values at the stop points A, B, C, H, J and K are higher than the others. This represents that these stop points are surrounded by the tall buildings which results the poor PVT services. The high GDOP value is caused by the signal blockage. Note that the highest GDOP value is at the stop point J, because three buildings around the stop point J which could block the signals from satellites with

medium or low elevation angles. Only the signals from high elevation satellites can be received which results the poor geometry for positioning. These places are considered as the radio frequency difficult environments. The stop point J is considered as the most radio frequency difficult environment for GPS, and this paper places the equipment at the stop point J and collects the GPS signal. The equipment utilized in this experiment is depicted in the Figure 4.

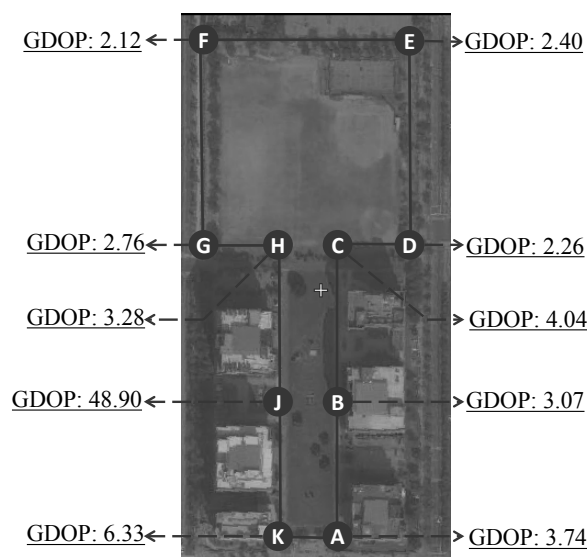


Figure 3 The test result of a commercial receiver, Garmin GPS 35. The receiver is stayed at each circle for 20 minutes to calculate the average GDOP

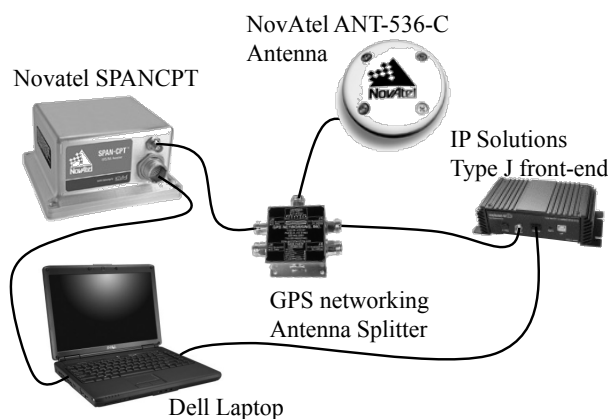


Figure 4 The configuration of the equipment used in this paper

The bandwidth, the intermediate frequency, and the sampling frequency of the IP Solutions front-end are 4 MHz, 4.123968 MHz, and 16.367667 MHz, respectively. This paper also uses a high accuracy GPS/INS integrated receiver, NovAtel SPAN-CPT receiver, as the truth of the positioning solutions. The signals are collected on

February 9, 2012, at 14:57 (UTC). There are two experiments conducted in this paper.

The first scenario is that all the signals are well received, and the other scenario is that the building blocks some of the signals for a short period of time. Figure 5 shows the comparison plots of the positioning results for the conventional receiver, the vector tracking receiver, and the NovAtel SPAN-CPT receiver under the first scenario, and one can note that the vector tracking receiver has the higher positioning accuracy than that of the conventional receiver. This is due to the vector tracking receiver takes advantage of the user dynamic to predict the user position, velocity, clock bias and drift. It is important to note that the vector tracking is capable of estimating precise code delay by combining the signal power from all channels which results that the tracking noise could be greatly reduced. Thus, the variance of the positioning error of a vector tracking receiver is lower than that of the conventional receiver. In other words, the positioning performance of the vector tracking receiver is also more accurate than that of the conventional receiver.

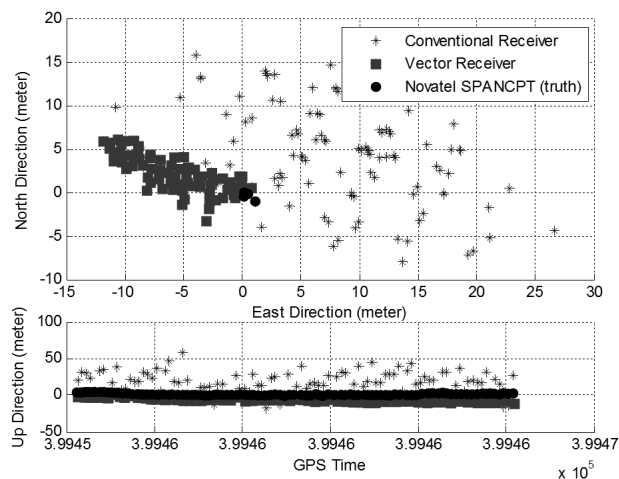


Figure 5 The comparison of positioning performance between conventional receiver, vector receiver, and Novatel SPAN-CPT

Table 1 summarizes the positioning results under the first scenario. The other benefit of the vector tracking receiver is the capability to bridge the short outage of the weak signal. This can be observed from the second scenario. Figure 6 shows the skyplot of the second scenario. To observe Figure 6, the south-east side of skyplot has only two satellites, and SV 24 is in a very low carrier to noise ratio ( $C/N_0$ ). Additionally, considering the impact on the geometric distribution for positioning (i.e., GDOP), the continuous tracking of the SV24 and SV 31 are crucial for good positioning performance. However, under this scenario, the conventional receiver would loss lock of the SV24 due to its low  $C/N_0$ .

Table 1 Positioning error mean and variance by using conventional and vector receiver

Unit: meter	Error mean	Error variance
Conventional receiver (E-N)	12.08	23.04
Conventional receiver (U)	18.55	141.57
Vector receiver (E-N)	6.74	12.26
Vector receiver (U)	6.59	8.55

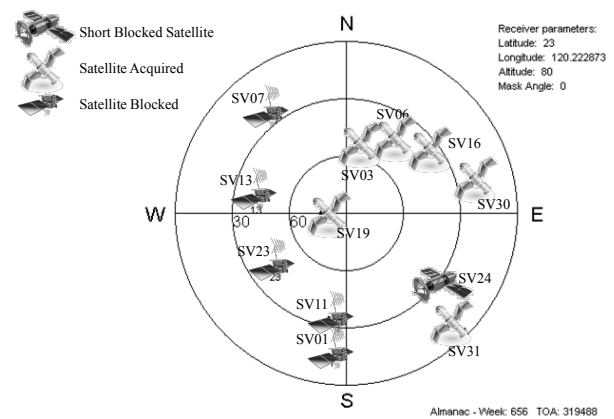


Figure 6 The skyplot of scenario 2

As shown in Figure 7, the threshold for the  $C/N_0$  value to be declared as tracked is set to be 25 dB-Hz which is determined by the empirical experience. This paper applies the power ratio method of [10] to calculate the  $C/N_0$  values. As indicated in Figure 7, the conventional tracking loop design fails to keep tracking the signal roughly from epoch 17,000. The bottom plot of Figure 7 shows that the  $C/N_0$  of SV24 for the conventional tracking loop design is too low to be locked. On the contrary, although the vector tracking loop design undergoes the same attenuated signal of SV24, it could continue the good positioning services even there is temporary outage. The upper plot of Figure 7 indicates that the vector tracking loop could still lock the attenuated signal of SV24. The result demonstrates that the main benefit of the vector tracking loop. Furthermore, the  $C/N_0$  estimated by the vector tracking loop is slightly higher than that of the conventional tracking loop. In addition, the noise calibration method of the Kalman filter in the above discussions is based on the empirical tuning method.

#### Analysis of Noise Calibration Methods

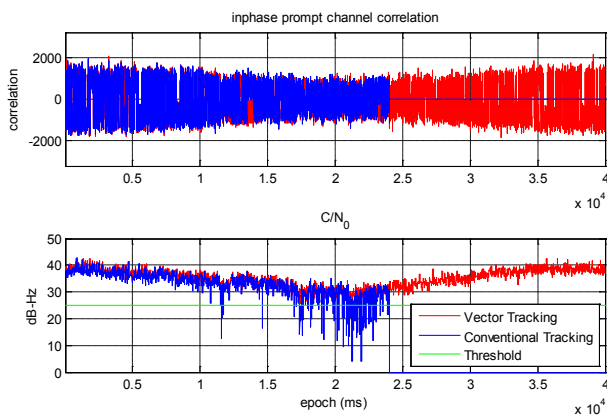
The measurement noise covariance of the empirical tuning method is summarized in Table 2. As shown in Table 2, the code measurement noise variances are the same in all channels, that is,  $400 \text{ m}^2$ . This feature denotes that all channels are believed to be equally weighted. However, it is generally against the truth.

Table 2 The measurement, the process noise covariance, and the initial state error covariance applied in this paper by the empirical tuning method

Measurement Noise Covariance $R$			
Code phase error $\sigma^2(m^2)$ 400		Carrier frequency error $\sigma^2(m^2/s^2)$ 100	
Initial State Error Covariance $P$			
Position error $\sigma^2(m^2)$ 2	Velocity error $\sigma^2(m/s^2)$ 0.5	Clock bias $\sigma^2(m)$ 0.2	Clock drift $\sigma^2(m/s^2)$ 1e-5
Process Noise Covariance $Q$			
Position error $\sigma^2(m^2)$ 20	Velocity error $\sigma^2(m/s^2)$ 10	Clock bias $\sigma^2(m)$ 4.3e-9	Clock drift $\sigma^2(m/s^2)$ 0.005

Table 3 The measurement, and process noise covariance applied in this paper by the correlation method

Measurement Noise Covariance $R$													
Code phase error $\sigma^2$ of each channel ( $m^2$ )							Carrier frequency error $\sigma^2$ of each channel ( $m^2/s^2$ )						
Ch.1	Ch.2	Ch.3	Ch.4	Ch.5	Ch.6	Ch.7	Ch.1	Ch.2	Ch.3	Ch.4	Ch.5	Ch.6	Ch.7
413	651	393	734	2486	601	336	11	16	9	19	101	16	10
Process Noise Covariance $Q$													
Position error $\sigma^2(m^2)$			Velocity error $\sigma^2(m/s^2)$			Clock bias $\sigma^2(m)$			Clock drift $\sigma^2(m/s^2)$				
3.7	4.2	6.7	0.38	0.34	0.71	2.7e-7			1.5e-5				


 Figure 7 An example of bridging the short outage by the vector tracking technique. The green line is threshold of  $C/N_0$ 

In addition, the process noise covariance remains the same in the empirical tuning method, which is also not flexible to a mission with complicated motion. Based on these reasons, the performance of the empirical tuning method is limited. The mean and variance of the position error of the empirical tuning method are 4.7 meter and  $1.48 m^2$ , respectively. To observe Table 3, code measurement noise variances depends on the quality of signal. It is interesting to note that the mean and variance of the position error of the correlation method are 3.36 m and  $0.47 m^2$ , respectively. The positioning results of the correlation method are better than that of the empirical

tuning method. In order to verify the performance gain of the correlation method, the value of the noise covariance estimated by the correlation method is listed in Table 3.

It is interesting to note that the measurement variances are different for different channels, because the correlation method correlates the system outputs to determine the weightings for all measurements. As shown in Table 3, the variance of the code measurement of the fifth channel is much higher than the others, and the fifth channel tracks SV24 which is discussed in previous subsection, in other words, it successfully tracks the attenuated signal of SV24. By the correlation method, the code measurement from the fifth channel has less influence on the estimation. As a result, the performance gain from the correlation method is verified.

## V. CONCLUSIONS

An advanced GPS receiver technique, the vector tracking technique, was introduced in this paper. This paper implemented the vector delay lock loop (VDLL) to maintain the positioning performance when the GPS receiver was placed into a radio frequency difficult environment. This paper then utilized a commercial receiver to survey the selected experiment field, and regarded this field as the radio frequency difficult environment. The experiment results demonstrate that the vector receiver is capable of bridging the short outage of the GPS signal. As shown in the results, the vector tracking has more accurate positioning performance than that of the conventional receiver. This paper also

introduced two noise calibration methods, the empirical tuning method and the correlation method. According to the experiment results, the correlation method could capture more characteristics of signals and uses these characteristics to facilitate the vector tracking receiver.

### ACKNOWLEDGMENTS

The authors gratefully acknowledge Dr. Paul Groves for his thoughtful comments. The authors also thank Mr. Chien-Ho Chen, who helped the authors to collect the GPS signals used in this paper. The work presented in this paper is supported by Taiwan National Science Council under research grant, NSC 101-2628-E-006-013-MY3. The authors also thank NCKU Research and Development Foundation for providing the travel fund to MMT conference 2013.

### REFERENCES

- [1] Global GPS Market: Products (Marine, Aviation, Automotive, Outdoor/fitness & GPS Enabled Smart Phones), Applications (Navigation, Machine Control, & Logistics Tracking) & Geography (2011-2016), MarketsandMarkets online Publishers (2011). Available at <http://www.marketsandmarkets.com/Market-Reports/global-GPS-market-and-its-applications-142.html>
- [2] Li, B., Dempster, A. G., and Rizos, C., "Positioning in environments where GPS fails," *Surveying & XXIV FIG Int. Congress (2010)*, Sydney, Australia, 11-16 April.
- [3] Parkinson, B. W. and Spilker, J. J., "Global Positioning System: Theory and Application," American Institute of Aeronautics and Astronautics, 1996.
- [4] Pany, T., Kaniuth, R., and Eissfeller, B., "Deep Integration of Navigation Solution and Signal Processing," *Proceedings of the 18th ION GNSS International Technical Meeting of the Satellite Division*, Long Beach, CA, 2005.
- [5] Zhao, S. and Akos, D., "An Open Source GPS/GNSS Vector Tracking Loop - Implementation, Filter Tuning, and Results," *Proceedings of the 2011 International Technical Meeting of The Institute of Navigation*, San Diego, CA, 2011, pp. 1293-1305.
- [6] Kaplan, E. D., *Understanding GPS: Principles and Application*, Artech House Publishers, Boston, MA, 1996.
- [7] Groves, P. D., *Principles of GNSS, Inertial, and Multi-Sensor Integrated Navigation Systems (GNSS Technology and Applications)*, Artech House Publishers, 2007.
- [8] Pany, T., *Navigation Signal Processing for Gns Software Receivers (Gns Technology and Applications)*, Artech House, January 2010.
- [9] Mehra, R., "On-line identification of linear dynamic systems with applications to Kalman filtering, Automatic Control," *IEEE Transactions on*, Vol. 16, No. 1, February 1971, pp. 12-21.
- [10] Sharawi, M. S., Akos, D. M., and Aloï, D. N., "GPS C/N0 estimation in the presence of interference and limited quantization levels, Aerospace and Electronic Systems," *IEEE Transactions on*, Vol. 43, No. 1, January 2007, pp.227-238.